学位論文

Neuroprotective effect of water-dispersible hesperetin in retinal ischemia reperfusion injury

（網膜虚血再灌流障害における分散ヘスペレチンの神経保護効果）

旭川医科大学大学院医学系研究科博士課程医学専攻

下内　昭人

（横田陽匡、大野晋治、松本千恵美、玉井敏博、宅見央子、Subbadra P. Narayanan、
木村昭治、小林博也、Ruth B. Caldwell、長岡泰司、吉田晃敏）

Neuroprotective effect of water-dispersible hesperetin in retinal ischemia reperfusion injury

Running Title: WD-Hpt prevents retinal neuronal injury

Akito Shimouchi[1], Harumasa Yokota[1], Shinji Ono[1], Chiemi Matsumoto[1], Toshihiro Tamai[3], Hiroko Takumi[3], Subbadra P Narayanan[4], Shoji Kimura[2], Hiroya Kobayashi[2], Ruth B. Caldwell[4], Taiji Nagaoka[1], Akitoshi Yoshida[1],

From the [1]Department of Ophthalmology and [2]Department of Pathology, Division of Immune Pathology, Asahikawa Medical University, Asahikawa, Japan; and [3]Institute of Health Sciences, Ezaki Glico Co., Ltd, Osaka, Japan; and the [4]Vascular Biology Center, Georgia Regents University, Augusta, Georgia.

Corresponding author; Harumasa Yokota

Department of Ophthalmology, Asahikawa Medical University, Asahikawa, Midorigaoka Higashi 2-1-1-1, Asahikawa, 078-8510, Japan, Tel: 0166-68-2543, Fax: 0166-68-2549, e-mail: atokoy18@asahikawa-med.ac.jp

Abstract

Purpose To determine whether water-dispersible hesperetin (WD-Hpt) can prevent degeneration of ganglion cell neurons in the ischemic retina.

Methods Ischemia reperfusion (I/R) injury was induced by increasing the intraocular pressure of mice to 110 mmHg for 40 min. Mice received daily intraperitoneal injections with either normal saline (NS, 0.3 ml/day) or WD-Hpt (0.3 ml, 200 mg/kg/day). Reactive oxygen species (ROS) was assessed by dihydroethidium and nitrotyrosine formation. Inflammation was estimated by microglial morphology in the retina. Lipopolysaccharide (LPS)-stimulated BV-2 cells were used to explore the anti-inflammatory effect of WD-Hpt on activated microglia by quantifying the expression of IL-1β using real-time quantitative reverse transcription-polymerase chain reaction. Ganglion cell loss was assessed by immunohistochemistry of NeuN. Glial activation was quantified with glial fibrillary acidic protein (GFAP) immunoreactivity. Apoptosis was evaluated with a terminal deoxynucleotidyl transferase (TUNEL) assay and immunohistochemistry of cleaved caspase-3. Phosphorylation of extracellular signal-regulated kinase (p-ERK) was surveyed by western blotting.

Results WD-Hpt decreased I/R induced ROS formation. WD-Hpt alleviated microglial activation induced by I/R and reduced mRNA levels of IL-1β in LPS-stimulated BV-2. I/R resulted in a 37 % reduction in the number of ganglion cells in the NS-treated mice, whereas the reduction was only 5 % in the WD-Hpt-treated mice. In addition, WD-Hpt mitigated the immunoreactivity of GFAP, increased expression of cleaved caspase-3, increased number of TUNEL positive cells and p-ERK after I/R.

Conclusions WD-Hpt protected ganglion cells from I/R injury by inhibiting oxidative stress and modulating cell death signaling. Moreover, WD-Hpt had an anti-inflammatory effect through the suppression of activated microglia.

Keywords hesperetin・ischemia-reperfusion・neuroprotection・retina・inflammation

Introduction

Retinal ischemia is common among several major vision-threatening diseases including diabetic retinopathy (DR), retinopathy of prematurity and retinal vein occlusion. Although these retinopathies are diagnosed primarily by their vascular abnormalities such as avascular area, vascular leakage and retinal neovascularization, several clinical and experimental studies demonstrate the presence of inflammation [1-3], glial activation [4-6], and neurodegeneration [7, 8] in the retina before the appearance of typical vascular pathology. These studies suggest that ischemia-induced inflammation and neurotoxicity may play a pathophysiological role in mediating elements of the vascular pathology. From this point of view, protection of neuronal cells from ischemic retinopathy may offer a new strategy to prevent the development of vascular lesions.

Oxidative stress is critically involved in neuronal cell death in ischemic retinopathy [9-11]. It causes diverse pathways such as inflammation [12, 13], proliferation [14] and apoptosis [15]. The ganglion cell layer (GCL) is mostly affected during ischemia, as the layer is absolutely adjacent to the superficial vascular layer. Inflammation and apoptosis are typical pathological changes in the GCL layer in ischemic retinopathy [16]. A recent study of patients with type 1 diabetes using high-resolution optical coherence tomography (OCT) depicts thinning of the GCL that was closely correlated with the duration of diabetes even when DR was minimal [17]. This study also suggests a need for therapeutic intervention to prevent neuronal lesion in ischemic retinopathy.

Hesperetin (Hpt) is an aglycon of hesperidin, one of flavonoids, abundantly present in the skins of oranges. It is reported that Hpt has various beneficial effects including anti-oxidative[18], anti-inflammatory[19], anti-viral[20] and anti-carcinogenic [21, 22]. In addition, a recent experimental study demonstrates that Hpt can also prevent diabetes-induced gliosis, and vascular permeability in the retina [23]. However, whether Hpt can arrest neuronal degeneration in ischemic retinopathy remains obscure.

Water-dispersible hesperetin (WD-Hpt) has been recently introduced to enhance the bioavailability of Hpt into the tissues. WD-Hpt is the micronized product of Hpt with high dispersibility in liquid, thereby proven to attain a higher bioavailability compared to conventional Hpt [24]. The present study was conducted to investigate whether WD-Hpt can protect ganglion cells in ischemic retinopathy. Our data demonstrated that WD-Hpt markedly reduced oxidative stress, microglial activation and apoptosis in ischemic

retinopathy. This study further suggests that WD-Hpt can be used as a new therapeutic strategy for treating ischemic retinopathies such as DR.

Methods

Induction of retinal ischemia reperfusion (I/R) injury in mice

All procedures with animals were performed in accordance with the ARVO statement for the use of animals in ophthalmic and vision research and were approved by the institutional animal care and use committee (IACUC). All surgery was performed under anesthesia, and all efforts were made to minimize suffering. Transient retinal ischemia applied to wild type C57BL/6 mice. Mice were anesthetized with tribromomethanol (Avertin, 0.5 g/kg, intraperitoneally), pupils were dilated with 0.5 % tropicamide and 0.5 % phenylephrine, and topical anesthesia (1 drop of proparacaine hydrochloride was applied to cornea). The anterior chamber of the right eye was penetrated with a 30-gauge needle attached to a line infusing sterile saline. The intraocular pressure (IOP) was raised to 110 mmHg by elevating the saline reservoir up to 150 cm above the eye. Ischemia was confirmed by whitening of the anterior segment of the globe and blanching of the episcleral veins [25]. After 40 min of ischemia, the needle was withdrawn, and reperfusion was confirmed by observation of the episcleral veins. The left eyes were kept as controls. In a previous study the mice were killed at various times after I/R [26], and their retinas were prepared as described below; this practice was followed in the present study.

Water-dispersible hesperetin treatment for I/R

Water-dispersible hesperetin (WD-Hpt) was gifted from the Institute of Health Sciences, Ezaki Glico Co., Ltd, Osaka, Japan. WD-Hpt was diluted with sterilized water and injected intraperitoneally 30 min before the surgery and again once daily (0.3 ml, 200 mg/kg/day) until sacrifice. The dose of WD-Hpt was determined by following a previous study [27]. The other mice received normal saline (NS, 0.3 ml) as control.

Reactive oxygen species formation

Superoxide production was evaluated in retinal frozen sections collected at 6 h after I/R by the dihydroethidium (DHE) method, as described previously [28, 29]. Briefly, frozen

sections were stained with DHE (2 μM) for 20 min at 37 °C. DHE is oxidized on reaction with superoxide to form ethidium bromide, which binds to DNA in the nucleus and fluoresces red [30]. DHE images were obtained using a fluorescence microscope (Olympus, Tokyo, Japan). DHE was excited at 488 nm with an emission spectrum of 610 nm. Control and experimental tissues were placed on the same slide and processed under the same conditions. The settings for image acquisition were identical for the control and experimental tissues. The images were analyzed for reaction intensity using existing tools in the image processing software Photoshop (Adobe, St. Jose, CA., USA) [31]. Peroxynitrite ($ONOO^-$) is a short-lived molecule at physiological pH, but it has been shown to emit nitrate protein tyrosine residues. Therefore, $ONOO^-$ formation was indirectly detected by western blot analysis with a monoclonal anti-nitrotyrosine antibody (Cayman Chemical Co., Ann Arbor, MI, USA).

Evaluation of neuronal cell loss

Cell death was quantified by terminal deoxynucleotidyl transferase (TUNEL) assay (Roche Diagnostics, Indianapolis, IN., USA) using cryosection (10 μm) prepared from retinas collected 3 days after I/R, according to the manufacture's protocol. TUNEL-positive cells in each sample were counted manually on whole retinal sections extending from the optic disc to the ora serrata. The number of TUNEL-positive cells was averaged by using at least five sections (20 μm apart) per animal.

Surviving neurons within the ganglion cell layer (GCL) were quantified by confocal imaging of the GCL in retinal whole-mount preparations labeled with the neuronal cell marker NeuN. Eyes were collected at 7 days after I/R surgery and were fixed overnight in 4 % paraformaldehyde (PFA) in phosphate-buffered saline (PBS) at 4 °C. The retinas were dissected, washed with PBS, permeabilized with 10 % Triton (1 h), and incubated in blocking solution (1 % Triton, 10 % normal goat serum in PBS, 30 min). The retinas were incubated overnight at 4 °C with anti-NeuN conjugated with Alexa Fluor 488 (1:400; rabbit; Millipore, Temecula, CA, USA). After washing with PBS, flat-mounting, and covering with a cover slip, a confocal microscope (Olympus) was used to capture a group of five serial confocal images of the NeuN-positive GCL neurons separated by 1 μm. The images were then merged to generate one well-focused image. Ten images were taken in the mid-periphery of each retina using a 20× objective lens. The cells were

counted using ImageJ software (developed by Wayne Rasband, National Institutes of Health, Bethesda, MD, USA; available at http://rsb.info.nih.gov/ij/index.html) after image thresholding and manual exclusion of artifacts. The number of NeuN-positive cells in the GCL in I/R eyes was expressed as a ratio to the number in the contralateral control eyes in the same manner as a previous study [32].

Immunohistochemistry

Eyes were enucleated, fixed in 4 % PFA (overnight, 4 °C), and washed in PBS, and retinas were isolated and cryoprotected in 30 % sucrose. Cryostat sections (10 μm) were collected, permeabilized with 1 % Triton (20 min), and blocked in 10 % normal goat serum (1 h). Sections were then incubated overnight at 4 °C with the primary antibody glial fibrillary acidic protein (GFAP) conjugated with Cy3 (1:200; Sigma Aldrich, Saint Louis, Mo, USA), tubulin B3 (1:300; Mouse; Millipore), cleaved caspase-3 (1:100; rabbit; Cell Signaling Technology Inc., Danvers, MA, USA) or Iba1 (1:200; rabbit; Wako, Osaka, Japan). The nuclei were stained with 4', 6-diamidino-2-phenolindole (DAPI), and incubated on the following day (1 h) in goat anti-mouse IgG conjugated with FITC (1:400; Santa Cruz Biotechnology Inc., Dallas, Texas, USA) or goat anti-rabbit IgG conjugated with Rhodamine (1:400; Biomedical Technologies Inc., Stoughton, MA, USA) or goat anti-rabbit IgG conjugated with Alexia Fluor 647 (1:1000; Cell Signaling Technology) secondary antibody, washed in PBS, and mounted with mount medium (Vectorshield; Vector Laboratories, Burlingame, CA, USA).

Western blot analysis

Retinal homogenates were prepared using RIPA buffer (Millipore) containing protease and phosphatase inhibitors (Complete Mini and phosSTOP, respectively; Roche Applied Science, Indianapolis, IN, USA). Proteins were separated on SDS-PAGE and transferred onto nitrocellulose membranes (Millipore), blocked in 5 % milk or 3 % BSA in TBST (Tris-buffered saline with 0.5 % Tween-20). The membranes were incubated overnight at 4 °C with primary antibodies diluted in blocking solution consisting of total extracellular signal-regulated kinase (t-ERK; Thr202/Tyr204; 1:5000; rabbit; Cell Signaling Technology), phosphorylation of ERK (p-ERK; 1:5000; rabbit; Cell Signaling Technology), GFAP (1:1000; rabbit; Sigma-Aldrich), tubulin (1:10,000; mouse;

Sigma-Aldrich) or actin (1:1000; mouse; Cell Signaling Technology). The next day, the membranes were washed in TBST, followed by horseradish peroxidase-conjugated secondary antibody (1:2000 or 1:5000; rabbit or mouse; GE Healthcare, London, England, UK). Immunoreactive proteins were detected using the enhanced chemiluminescence system (GE Healthcare Bio-Science Corp., Piscataway, NJ, USA).

Cell culture

BV-2 is a widely used cell line of murine microglia and considered to be suitable for in vitro study of microglia [33, 34]. BV-2 cells were cultured at 37 °C with 5 % CO_2 in Medium [RPMI1640 (fetal bovine serum (FBS) free; nacalai tesque, Kyoto, Japan) supplemented with 10 % FBS (Thermo Fisher Scientific, Yokohama, Japan), 100 μg/ml streptomycin (nacalai), 1 mM sodium pyruvate (nacalai) and 100 U/ml penicillin (nacalai)]. Cells at 1×10^5 cells per well were plated into flat-bottom 24-well plates and either treated or untreated with hesperetin 3'-O-beta-D-glucuronide, a metabolic form of WD-Hpt in the circulation, at final concentrations of 0, 10 or 100 μM (gifted from Ezaki Glico, Osaka, Japan) maintained at 37 °C and 5 % CO_2 for 1 h. The cells were stimulated by incubation with lipopolysaccharide (LPS) at final concentrations of 100 ng/ml for 4 h in a 5 % CO_2 incubator at 37 °C [35].

Quantitative real-time qRT-PCR

Total RNA was isolated from BV-2 cells with NucleoSpin RNA XS (74902, TaKaRa Bio Inc., Kusatsu, Japan) according to the manufacturer's instructions. Total RNA (0.5 μg) was reverse-transcribed into cDNA using a transcripter first strand cDNA synthesis kit (4379012, Roche). Messenger RNA (mRNA) abundance was determined by real-time quantitative reverse transcription polymerase chain reaction (qRT-PCR) with LightCycler 480 SYBR Green I master (4707516, Roche) and specific primer sets. Data were collected and quantitatively analyzed with LightCycler 480 real-time PCR system (Roche) (95 °C; 10 s, 55 °C; 22 s, 72 °C; 5 s, 45 cycles). Gene expression was assessed by normalizing to β-actin. The PCR primers used in this study are listed below: forward strand IL-1β, 5'-AGTTGACGGACCCCAAAAG-3'; reverse strand IL-1β, 5'-AGCTGGATGCTCTCATCAGG-3'; forward strand β-actin, 5'-

CTAAGGCCAACCGTGAAAAG -3'; reverse strand β-actin, 5'-ACCAGAGGCATACAGGGACA -3'.

Statistical analysis

Results were expressed as mean ± SEM. Statistical analysis was performed with one-way ANOVA followed by a Tukey test for multiple comparisons. In the case of single comparison, the Student's *t*-test was applied. $P < 0.05$ was considered statistically significant.

Results

Effect of WD-Hpt on oxidative stress in the retina

Studies show that oxidative stress is a key player in retina neuronal injury in models of I/R [9-11]. To test whether WD-Hpt could reduce oxidative stress in I/R retina, we assessed formation of the peroxinitrite biomarker nitrotyrosine at 6 h after I/R by western blot analysis. This analysis showed a robust increase of nitrotyrosine immunoreactivity in the I/R retina treated with NS (NS I/R) (Fig. 1a). However, a reduction of the increased nitrotyrosine immunoreactiveity was observed in the I/R retina treated with WD-Hpt (WD-Hpt I/R). Furthermore, DHE staining was performed to assess a beneficial inhibitory effect of WD-Hpt on superoxide formation in the retina at 6 h after I/R. The DHE-superoxide reaction was also prevented by the WD-Hpt treatment. Fig. 1b shows representative images of quantitative analysis of the DHE reaction. Imaging of the NS I/R retina showed increased DHE reaction, especially in the ganglion cell layer (GCL) and inner nuclear layer (INL).

Effect of WD-Hpt treatment on microglia and reduction of retinal IL-1β levels

Reactive oxygen species (ROS) triggers retinal inflammation in ischemic retinopathy [36, 37]. Microglia should be activated while retinal inflammation continues following I/R insults [38, 39]. Therefore, we evaluated microglial activation from microglial morphology in the current study. We visualized microglia in the retina by means of immunohistochemistry with the microglial marker Iba1. Microglia generally show a small cell body with numbers of long-branched processes when they are in a resting state. Once microglia activate, their cell bodies become large with shorter processes compared to a resting state [40-42]. As expected, at 24 h after I/R, microglia became active, displaying shorter processes and a large cell body. In contrast, compared to the NS I/R retina, the microglia seemed to have relatively longer processes and a smaller cell body in the WD-Hpt I/R retina (Fig. 2a).

Microglia mediate inflammation by releasing a wide variety of inflammatory cytokines [43-45]. In the present study, we used LPS-stimulated BV-2 cells releasing IL-1β to see whether WD-Hpt could prevent an increased production of inflammatory

cytokines from activated microglia [33, 34]. Quantitative real-time PCR analysis demonstrated that LPS stimulation resulted in a 3.5-folds increase in the mRNA levels of IL-1β (Fig. 2b). The expression of IL-1β in the BV-2 cells treated with 10 μM of Hpt 3'-O-beta-D-glucuronide was 3.0 folds higher compared with the control. However, 100 μM of Hpt 3'-O-beta-D-glucuronide reduced the increased expression levels of IL-1β to 1.7-folds of the control.

Reduction in retinal cell death, improved neuronal cell survival and reduced glial activation by WD-Hpt

Loss of neuronal cells within the GCL is a hallmark of retinal I/R injury [16]. A reduction in the increased expression of inflammatory cytokine should lead to the protection of ganglion cells in the I/R retina. To test this, we performed confocal imaging to quantify the number of NeuN-positive cells within the GCL in the flat-mounted retinas at 7 days after I/R (Fig. 3). This analysis demonstrated that the number of GCL neurons in the NS I/R retina was markedly reduced by I/R injury as compared with the contralateral control retinas, whereas the density of GCL neurons in the WD-Hpt I/R mice was nearly close to that in the contralateral eyes. The quantification of the surviving GCL neurons in the NS I/R retina showed a 37 % decrease relative to the control. By contrast, in the WD-Hpt I/R retina the decrease was only 5 % ($P < 0.01$).

Glial activation is another prominent feature of retinal I/R injury, diabetic retinopathy and other forms of ischemic retinopathy [4-6]. To see whether WD-Hpt can alleviate this aspect of retinal injury, we examined the expression of GFAP, known to increase during glial activation. As shown in Fig. 4a, the immunoblotting demonstrated that, compared with the contralateral control eyes, GFAPs were markedly increased in the NS I/R retina. By contrast, GFAP levels in the WD-Hpt I/R retina were almost comparable to those in the control retina. In addition, GFAP immunoreactivity in the NS I/R retina was localized to filamentous processes in the nerve fiber layer to the outer limiting membrane, corresponding to the distribution of astrocytes and Müller cells (Fig. 4b). GFAP immunolabeling in the radial Müller cell processes in the WD-Hpt I/R retina was much weaker than in the NS I/R retina, suggesting that WD-Hpt reduced glial injury in the I/R retina.

Reduction of I/R-induced apoptosis by WD-Hpt

Oxidative stress initiates an intrinsic apoptotic pathway leading to neuronal cell death in the I/R retina [46]. To see whether WD-Hpt was able to reduce apoptosis in the I/R retina, we performed immunohistochemistry of tubulin B3 (neuron-specific marker) and cleaved caspase-3 at 24 h after I/R, and TUNEL staining at 3 days after I/R. As shown in Fig.5, the expression of cleaved caspase-3 was increased exclusively in the GCL and INL layers of the I/R retina. Similarly, TUNEL-positive cells were also present in the GCL and INL layers of I/R retina (Fig. 6). This was also alleviated by WD-Hpt treatment.

Effect of WD-Hpt on mitogen-activated protein kinases (MAPKs) in the retina

Phosphorylation of MAPKs, such as extracellular signal-regulated kinases (ERKs), is reported during retinal I/R [47]. MAPKs are redox sensitive, and inhibition of ERKs is reported to limit neurodegeneration in ischemic retinopathy [47]. Thus, we performed western blot analysis to see whether WD-Hpt could reduce MAPK activation. The analysis showed that levels of phosphorylated ERKs (p-ERKs) were markedly increased at 6 h after I/R. The increase of p-ERKs by I/R was significantly attenuated by WD-Hpt treatment (Fig. 7).

Discussion

In the present study, we tested the effect of WD-Hpt on ganglion cell death in a model of ischemic retinopathy. Our results showed that WD-Hpt could reduce the generation of ROS, inflammation and apoptosis signaling related to the ganglion cell death in the I/R retina. Moreover, hesperetin 3'-O-beta-D-glucuronide directly showed an anti-inflammatory effect via reduction in the increased expression of IL-1β from activated microglia. To the best of our knowledge, the present study is the first to prove a neuroprotective effect of WD-Hpt in the ischemic retinal diseases.

We previously reported that ROS generated by NADPH oxidase 2 (NOX2) plays an important role in ganglion cell death in an ischemia reperfusion (I/R) model [26]. It is reported that Hpt has powerful antioxidant effects that modulate enzymatic activities and ROS scavenging activities [18]. In the present study, using DHE imaging studies, we showed that WD-Hpt treatment significantly reduced superoxide formation in the I/R retina. Further, western blot analysis demonstrated elevated levels of nitrotyrosine, the peroxynitrite biomarker in NS I/R retinas, which was also considerably attenuated in the retina treated with WD-Hpt. These results suggest that WD-Hpt exhibited strong antioxidant activities in the ischemic retina.

Our data show for the first time that WD-Hpt alleviated the activation of microglia due to I/R. Microglia give rise to chronic inflammation by releasing a wide variety of inflammatory cytokines in the retinal pathologies, including I/R retina and ischemia [35, 43-45, 48-50]. IL-1β is a major cytokine released from activated microglia. Kumar, et al. recently demonstrated that Hpt succeeded in mitigating the increased expression of IL-1β in the retinas of diabetic rodents [23]. However, they did not clarify that Hpt showed a beneficial inhibitory effect on activated microglia. Since LPS has been widely used to activate microglia through the Toll-like receptor 4 (TLR4) [51], we used a cultured microglia cell line of BV-2 stimulated by LPS in order to explore the inhibitory effect of WD-Hpt on activated microglia. Although we did not confirm the expression of TLR4 in the I/R retina, a previous study clearly demonstrates that TLR4 was also involved in retinal inflammation by I/R injury [52]. Thus, the results obtained from the experiment using LPS-stimulated BV-2 cells, which showed that WD-Hpt reduced the increased expression of IL-1β in activated microglia, properly supports the results obtained from the in vivo experiment demonstrating that WD-Hpt increased the ramification of the

microglia in the I/R retina. Therefore, it is suggested that WD-Hpt has not only an anti-oxidative but also an anti-inflammatory effect on ischemic retinopathy.

Many studies show that apoptosis is definitely involved in the process of ganglion cell death in ischemic retinopathy [16, 53-55]. Caspase-3 is known as a molecule that executes apoptosis in ischemic retinopathy [56-58]. In the present study, WD-Hpt attenuated the cleavage of procaspase-3 in the GCL and INL at 24 h after I/R. Kumar et al. also report that Hpt reduced the increased expression of caspase-3 in the cells of astrocytes and Müller cells, and the INL in diabetic rats [23]. Although the expression pattern of caspase-3 is variable among various models of experiments, these results suggest that WD-Hpt can attenuate neurodegenerative alterations in the retina by suppressing apoptosis in the neurons and glia. To further confirm if apoptotic cell death was reduced by WD-Hpt treatment, we performed TUNEL staining at 3 days after I/R. The current data for the first time demonstrated a reduction of I/R-induced apoptotic cell death in the GCL and INL by intraperitneal injection of WD-Hpt.

Gliosis is considered as a hallmark of retinal injury during disease states such as ischemia and diabetes. Increased immunoreactivity for GFAP is a well-known marker for gliosis and is evident especially in Müller cells [4-6]. Although I/R injury induces both glial activation and ganglion cell death, no study has so far elucidated a direct relationship between Müller cell activation and ganglion cell death. Instead of ganglion cell death, it is reported that retinal edema is attributed in part to gliosis in ischemic retinopathy [59, 60]. Our data show that WD-Hpt decreased the GFAP expression in Müller cells, suggesting that WD-Hpt alleviated glial activation in the I/R retina. This result indicates a capability of WD-Hpt to reduce retinal edema that causes a persistent visual deterioration in ischemic retinopathy. Therefore, it might be concluded that WD-Hpt application may lead to new therapy not only by preventing ganglion cell death but also in reducing macular edema that is highly prevalent in DR. A further study will need to be conducted to see if WD-Hpt is able to alleviate macular edema in ischemic retinopathy.

A previous study elucidated the role of ERK in retinal neuronal degeneration by the fact that MEK inhibitor U0126 could reverse a decrease in the thinning of the retina after I/R [61]. In the present study, WD-Hpt reduced the activation of ERK at 6 h after I/R. This seems to be one mechanism by which WD-Hpt protects ganglion cells from retinal I/R insult. In contrast to our results, Hpt is reported to exert neuroprotective effects

through an increase in phosphorylation of ERK in the culture cortical cells exposed to staurosporine [62]. Defining the role of ERK depends on the particular conditions employed in the studies and may, therefore, differ accordingly. Our previous study demonstrated that retinal I/R caused the activation of ERK and a deletion of NOX2, one main source of ROS in I/R injury in the retina, leading to a reduction in the activation of ERK. This indicates that the activation of ERK is in some way responsible for the ganglion cell death in ischemic retinopathy [26].

Our present study clearly demonstrates a promising neuroprotective effect of WD-Hpt in the ischemic retina. Further work, however, is needed to determine how to deliver WD-Hpt efficiently to the retina. In the present study, we utilized intraperitoneal injection of WD-Hpt to minimize variation of daily dosage. Therefore, the present data indicate systemic administration of WD-Hpt could be a treatment for targeting retinal diseases unless there are no severe adverse effects. In contrast, in the clinical treatment of eye diseases, local administration of drugs is most common. Application of eye drops is easier and safer compared to intravitreal injection that is employed in local administration, especially for ischemic retinopathies. Nevertheless, eye drops do not seem to achieve optimal concentration of a drug in the vitreous and retina and, therefore, at the moment there are no eye drops to treat ischemic retinopathy. Intravitreal injection could, therefore, be an alternative way of delivering WD-Hpt to the retina.

In summary, our present study suggests that WD-Hpt can protect ganglion cells from ischemic retinopathy through its anti-oxidative and anti-inflammatory effect. Ischemic retinopathies are initiated by a variety of stresses, including hyperglycemia, hypoxia, oxidative stress and inflammation. Taken together with previous reports, these results indicate that WD-Hpt can be effective for treating neuroinflammation in DR.

Acknowledgement

This work is supported by Grant in aid for Young Scientists (B) Grant 25861609 (HY) from the Ministry of Education, Science and Culture, Tokyo, Japan.

Conflicts of interest: A. Shimouchi, Grant (Ezaki Glico Co., Ltd.); H. Yokota, Grant (Ezaki Glico Co., Ltd.); S. Ono, None; C. Matsumoto, None; T. Tamai, Employee (Ezaki Glico Co., Ltd.); H. Takumi, Employee (Ezaki Glico Co., Ltd.); S. P. Narayanan, None; S. Kimura, None; H. Kobayashi, None; R. B. Caldwell, None; T. Nagaoka, None; A. Yoshida, None.

References

1. Joussen AM, Poulaki V, Le ML, Koizumi K, Esser C, Janicki H, et al. A central role for inflammation in the pathogenesis of diabetic retinopathy. FASEB J. 2004; 18:1450-2.
2. Esser P, Bresgen M, Fischbach R, Heimann K, Wiedemann P. Intercellular adhesion molecule-1 levels in plasma and vitreous from patients with vitreoretinal disorders. Ger J Ophthalmol. 1995; 4:269-74.
3. Nagai N, Izumi-Nagai K, Oike Y, Koto T, Satofuka S, Ozawa Y, et al. Suppression of diabetes-induced retinal inflammation by blocking the angiotensin II type 1 receptor or its downstream nuclear factor-kappaB pathway. Invest Ophthalmol Vis Sci. 2007; 48:4342-50.
4. Rungger-Brandle E, Dosso AA, Leuenberger PM. Glial reactivity, an early feature of diabetic retinopathy. Invest Ophthalmol Vis Sci. 2000; 41:1971-80.
5. Dyer MA, Cepko CL. Control of Muller glial cell proliferation and activation following retinal injury. Nat Neurosci. 2000; 3:873-80.
6. Yoshida S, Yoshida A, Ishibashi T. Induction of IL-8, MCP-1, and bFGF by TNF-alpha in retinal glial cells: implications for retinal neovascularization during post-ischemic inflammation. Graefes Arch Clin Exp Ophthalmol. 2004; 242:409-13.
7. Barber AJ, Lieth E, Khin SA, Antonetti DA, Buchanan AG, Gardner TW. Neural apoptosis in the retina during experimental and human diabetes. Early onset and effect of insulin. J Clin Invest. 1998; 102:783-91.
8. Villarroel M, Ciudin A, Hernandez C, Simo R. Neurodegeneration: An early event of diabetic retinopathy. World J Diabetes. 2010; 1:57-64.
9. Rios L, Cluzel J, Vennat JC, Menerath JM, Doly M. Comparison of intraocular treatment of DMTU and SOD following retinal ischemia in rats. J Ocul Pharmacol Ther. 1999; 15:547-56.
10. Nayak MS, Kita M, Marmor MF. Protection of rabbit retina from ischemic injury by superoxide dismutase and catalase. Invest

Ophthalmol Vis Sci. 1993; 34:2018-22.
11. Szabo ME, Droy-Lefaix MT, Doly M, Carre C, Braquet P. Ischemia and reperfusion-induced histologic changes in the rat retina. Demonstration of a free radical-mediated mechanism. Invest Ophthalmol Vis Sci. 1991; 32:1471-8.
12. Treins C, Giorgetti-Peraldi S, Murdaca J, Van Obberghen E. Regulation of vascular endothelial growth factor expression by advanced glycation end products. J Biol Chem. 2001; 276:43836-41.
13. Satofuka S, Ichihara A, Nagai N, Noda K, Ozawa Y, Fukamizu A, et al. (Pro)renin receptor-mediated signal transduction and tissue renin-angiotensin system contribute to diabetes-induced retinal inflammation. Diabetes. 2009; 58:1625-33.
14. Takeda M, Takamiya A, Yoshida A, Kiyama H. Extracellular signal-regulated kinase activation predominantly in Muller cells of retina with endotoxin-induced uveitis. Invest Ophthalmol Vis Sci. 2002; 43:907-11.
15. Zhou RH, Yan H, Wang BR, Kuang F, Duan XL, Xu Z. Role of extracellular signal-regulated kinase in glutamate-stimulated apoptosis of rat retinal ganglion cells. Curr Eye Res. 2007; 32:233-9.
16. Rosenbaum DM, Rosenbaum PS, Gupta H, Singh M, Aggarwal A, Hall DH, et al. The role of the p53 protein in the selective vulnerability of the inner retina to transient ischemia. Invest Ophthalmol Vis Sci. 1998; 39:2132-9.
17. van Dijk HW, Verbraak FD, Kok PH, Garvin MK, Sonka M, Lee K, et al. Decreased retinal ganglion cell layer thickness in patients with type 1 diabetes. Invest Ophthalmol Vis Sci. 2010; 51:3660-5.
18. Hirata A, Murakami Y, Shoji M, Kadoma Y, Fujisawa S. Kinetics of radical-scavenging activity of hesperetin and hesperidin and their inhibitory activity on COX-2 expression. Anticancer Res. 2005; 25:3367-74.
19. Galati EM, Monforte MT, Kirjavainen S, Forestieri AM, Trovato A, Tripodo MM. Biological effects of hesperidin, a citrus flavonoid. (Note I): antiinflammatory and analgesic activity. Farmaco. 1994; 40:709-12.

20. Kaul TN, Middleton E, Jr., Ogra PL. Antiviral effect of flavonoids on human viruses. J Med Virol. 1985; 15:71-9.
21. Zarebczan B, Pinchot SN, Kunnimalaiyaan M, Chen H. Hesperetin, a potential therapy for carcinoid cancer. Am J Surg. 2011; 201:329-32; discussion 33.
22. Garg A, Garg S, Zaneveld LJ, Singla AK. Chemistry and pharmacology of the Citrus bioflavonoid hesperidin. Phytother Res. 2001; 15:655-69.
23. Kumar B, Gupta SK, Srinivasan BP, Nag TC, Srivastava S, Saxena R, et al. Hesperetin rescues retinal oxidative stress, neuroinflammation and apoptosis in diabetic rats. Microvasc Res. 2013; 87:65-74.
24. Takumi H, Nakamura H, Simizu T, Harada R, Kometani T, Nadamoto T, et al. Bioavailability of orally administered water-dispersible hesperetin and its effect on peripheral vasodilatation in human subjects: implication of endothelial functions of plasma conjugated metabolites. Food Funct. 2012; 3:389-98.
25. Da T, Verkman AS. Aquaporin-4 gene disruption in mice protects against impaired retinal function and cell death after ischemia. Invest Ophthalmol Vis Sci. 2004; 45:4477-83.
26. Yokota H, Narayanan SP, Zhang W, Liu H, Rojas M, Xu Z, et al. Neuroprotection from retinal ischemia/reperfusion injury by NOX2 NADPH oxidase deletion. Invest Ophthalmol Vis Sci. 2011; 52:8123-31.
27. Shen J, Nakamura H, Fujisaki Y, Tanida M, Horii Y, Fuyuki R, et al. Effect of 4G-alpha-glucopyranosyl hesperidin on brown fat adipose tissue- and cutaneous-sympathetic nerve activity and peripheral body temperature. Neurosci Lett. 2009; 461:30-5.
28. Rojas M, Zhang W, Lee DL, Romero MJ, Nguyen DT, Al-Shabrawey M, et al. Role of IL-6 in angiotensin II-induced retinal vascular inflammation. Invest Ophthalmol Vis Sci. 2010; 51:1709-18.
29. Al-Shabrawey M, Bartoli M, El-Remessy AB, Platt DH, Matragoon S, Behzadian MA, et al. Inhibition of NAD(P)H oxidase activity blocks vascular endothelial growth factor overexpression and neovascularization during ischemic retinopathy. Am J Pathol. 2005; 167:599-607.

30. Miller FJ, Jr., Gutterman DD, Rios CD, Heistad DD, Davidson BL. Superoxide production in vascular smooth muscle contributes to oxidative stress and impaired relaxation in atherosclerosis. Circ Res. 1998; 82:1298-305.
31. Kirkeby S, Thomsen CE. Quantitative immunohistochemistry of fluorescence labelled probes using low-cost software. J Immunol Methods. 2005; 301:102-13.
32. Leahy KM, Ornberg RL, Wang Y, Zhu Y, Gidday JM, Connor JR, et al. Quantitative ex vivo detection of rodent retinal ganglion cells by immunolabeling Brn-3b. Exp Eye Res. 2004; 79:131-40.
33. Blasi E, Barluzzi R, Bocchini V, Mazzolla R, Bistoni F. Immortalization of murine microglial cells by a v-raf/v-myc carrying retrovirus. J Neuroimmunol. 1990; 27:229-37.
34. Luo C, Chen M, Xu H. Complement gene expression and regulation in mouse retina and retinal pigment epithelium/choroid. Mol Vis. 2011; 17:1588-97.
35. Tanaka T, Kai S, Matsuyama T, Adachi T, Fukuda K, Hirota K. General anesthetics inhibit LPS-induced IL-1beta expression in glial cells. PLoS One. 2013; 8:e82930.
36. Nagata M. Inflammatory cells and oxygen radicals. Curr Drug Targets Inflamm Allergy. 2005; 4:503-4.
37. Hordijk PL. Regulation of NADPH oxidases: the role of Rac proteins. Circ Res. 2006; 98:453-62.
38. Kaur C, Rathnasamy G, Ling EA. Roles of activated microglia in hypoxia induced neuroinflammation in the developing brain and the retina. J Neuroimmune Pharmacol. 2013; 8:66-78.
39. Arana L, Ordonez M, Ouro A, Rivera IG, Gangoiti P, Trueba M, et al. Ceramide 1-phosphate induces macrophage chemoattractant protein-1 release: involvement in ceramide 1-phosphate-stimulated cell migration. Am J Physiol Endocrinol Metab. 2013; 304:E1213-26.
40. Ling EA, Wong WC. The origin and nature of ramified and amoeboid microglia: a historical review and current concepts. Glia. 1993; 7:9-18.
41. Xu H, Chen M, Forrester JV. Para-inflammation in the aging retina.

Prog Retin Eye Res. 2009; 28:348-68.
42. Liu S, Li ZW, Weinreb RN, Xu G, Lindsey JD, Ye C, et al. Tracking retinal microgliosis in models of retinal ganglion cell damage. Invest Ophthalmol Vis Sci. 2012; 53:6254-62.
43. Colton CA, Gilbert DL. Production of superoxide anions by a CNS macrophage, the microglia. FEBS Lett. 1987; 223:284-8.
44. Banati RB, Rothe G, Valet G, Kreutzberg GW. Detection of lysosomal cysteine proteinases in microglia: flow cytometric measurement and histochemical localization of cathepsin B and L. Glia. 1993; 7:183-91.
45. Gehrmann J, Matsumoto Y, Kreutzberg GW. Microglia: intrinsic immuneffector cell of the brain. Brain Res Brain Res Rev. 1995; 20:269-87.
46. Bonne C, Muller A, Villain M. Free radicals in retinal ischemia. Gen Pharmacol. 1998; 30:275-80.
47. Roth S, Shaikh AR, Hennelly MM, Li Q, Bindokas V, Graham CE. Mitogen-activated protein kinases and retinal ischemia. Invest Ophthalmol Vis Sci. 2003; 44:5383-95.
48. Zhang C, Lam TT, Tso MO. Heterogeneous populations of microglia/macrophages in the retina and their activation after retinal ischemia and reperfusion injury. Exp Eye Res. 2005; 81:700-9.
49. Deng Y, Lu J, Sivakumar V, Ling EA, Kaur C. Amoeboid microglia in the periventricular white matter induce oligodendrocyte damage through expression of proinflammatory cytokines via MAP kinase signaling pathway in hypoxic neonatal rats. Brain Pathol. 2008; 18:387-400.
50. Rivera JC, Sitaras N, Noueihed B, Hamel D, Madaan A, Zhou T, et al. Microglia and interleukin-1beta in ischemic retinopathy elicit microvascular degeneration through neuronal semaphorin-3A. Arterioscler Thromb Vasc Biol. 2013; 33:1881-91.
51. Shimazu R, Akashi S, Ogata H, Nagai Y, Fukudome K, Miyake K, et al. MD-2, a molecule that confers lipopolysaccharide responsiveness on Toll-like receptor 4. J Exp Med. 1999; 189:1777-82.
52. Dvoriantchikova G, Barakat DJ, Hernandez E, Shestopalov VI, Ivanov

D. Toll-like receptor 4 contributes to retinal ischemia/reperfusion injury. Mol Vis. 2010; 16:1907-12.

53. Produit-Zengaffinen N, Pournaras CJ, Schorderet DF. Retinal ischemia-induced apoptosis is associated with alteration in Bax and Bcl-x(L) expression rather than modifications in Bak and Bcl-2. Mol Vis. 2009; 15:2101-10.

54. Zheng L, Gong B, Hatala DA, Kern TS. Retinal ischemia and reperfusion causes capillary degeneration: similarities to diabetes. Invest Ophthalmol Vis Sci. 2007; 48:361-7.

55. Lam TT, Abler AS, Tso MO. Apoptosis and caspases after ischemia-reperfusion injury in rat retina. Invest Ophthalmol Vis Sci. 1999; 40:967-75.

56. Doonan F, Cotter TG. Apoptosis: a potential therapeutic target for retinal degenerations. Curr Neurovasc Res. 2004; 1:41-53.

57. Zhang Y, Cho CH, Atchaneeyasakul LO, McFarland T, Appukuttan B, Stout JT. Activation of the mitochondrial apoptotic pathway in a rat model of central retinal artery occlusion. Invest Ophthalmol Vis Sci. 2005; 46:2133-9.

58. Parone PA, James D, Martinou JC. Mitochondria: regulating the inevitable. Biochimie. 2002; 84:105-11.

59. Wurm A, Iandiev I, Uhlmann S, Wiedemann P, Reichenbach A, Bringmann A, et al. Effects of ischemia-reperfusion on physiological properties of Muller glial cells in the porcine retina. Invest Ophthalmol Vis Sci. 2011; 52:3360-7.

60. Wurm A, Lipp S, Pannicke T, Linnertz R, Farber K, Wiedemann P, et al. Involvement of A(1) adenosine receptors in osmotic volume regulation of retinal glial cells in mice. Mol Vis. 2009; 15:1858-67.

61. Akiyama H, Nakazawa T, Shimura M, Tomita H, Tamai M. Presence of mitogen-activated protein kinase in retinal Muller cells and its neuroprotective effect ischemia-reperfusion injury. Neuroreport. 2002; 13:2103-7.

62. Rainey-Smith S, Schroetke LW, Bahia P, Fahmi A, Skilton R, Spencer JP, et al. Neuroprotective effects of hesperetin in mouse primary

neurones are independent of CREB activation. Neurosci Lett. 2008; 438:29-33

Fig. 1

Reduction of ischemia reperfusion (I/R)-induced reactive oxygen species (ROS) formation by water-dispersible hesperetin (WD-Hpt). **a** Western blot analysis of nitrotyrosine formation in the I/R retinas treated with normal saline (NS) or WD-Hpt. I/R increased the nitrotyrosine formation in mice treated with NS. This effect was reduced by WD-Hpt treatment ($n = 3$; $^{**}P < 0.01$ vs NS control (con); †$P < 0.05$ vs NS I/R). **b** The dihydroethidium (DHE) imaging of superoxide formation at 6 h after I/R. WD-Hpt reduced I/R-induced DHE reaction ($n = 6$; $^{**}P < 0.01$ vs NS con; ††$P < 0.01$ vs NS I/R). *GCL* ganglion cell layer, *IPL* inner plexiform layer, *INL* inner nuclear layer, *OPL* outer plexiform layer, *ONL* outer nuclear layer. *Scale bar* 50 μm.

Fig. 2

The inhibitory effect of WD-Hpt on activated microglia. **a** Fluorescent microscopic imaging of retinal sections labeled with Iba1, microglial marker, at 24 h after I/R. I/R resulted in microglia with a large cell body and shorter processes (NS I/R) compared to microglia with a small cell body and longer process in control retina (NS con). WD-Hpt mitigated the alteration of the morphology of microglia in I/R retina (WD-Hpt I/R). *Scale bar* 200 μm (*left line*) and 50 μm (*middle line*). **b** Expression of IL-1β in BV-2 cells stimulated by lipopolysaccharide (LPS). Hpt reduced increased expression of IL-1β at a concentration of 100 μM. Total RNA was extracted and IL-1β mRNA levels were assayed by real-time quantitative reverse transcription polymerase chain reaction (qRT-PCR) ($n = 3$; $^{*}P < 0.05$ vs con; †$P < 0.05$ vs LPS).

Fig, 3

Protective effect of WD-Hpt on neuronal cell in the GCL during I/R. Confocal imaging of flat-mounted retina labeled with NeuN antibody at 7 days after I/R shows a significant decrease in density of NeuN-positive cells in the GCL of the NS I/R retina compared with the NS con retina. WD-Hpt treatment significantly decreased the loss of NeuN-positive GCL neurons after I/R ($n = 4$; $^{**}P < 0.01$ vs NS con; ††$P < 0.01$ vs NS I/R). *Scale bar* 100 μm.

Fig. 4

The mitigation of glial activation by WD-Hpt in the retina during I/R injury. **a** Western blot analysis shows the increase of glial fibrillary acidic protein (GFAP) at 5 days after I/R, which

was reduced by WD-Hpt treatment (+, I/R treated groups, $n = 4$ for each of the treatments; −, control, $n = 3$ for each of the treatments; $^{**}P < 0.01$ vs NS con; †$P < 0.05$ vs NS I/R). **b** Immunohistochemistry analysis of retinal sections labeled with GFAP. *GCL* ganglion cell layer, *IPL* inner plexiform layer, *INL* inner nuclear layer, *OPL* outer plexiform layer, *ONL* outer nuclear layer. *Scale bar* 50 μm.

Fig. 5

Effect of WD-Hpt on apoptotic molecules during I/R retina. Fluorescent microscopic imaging of retinal sections labeled with tubulin B3 and cleaved caspase-3. High expression of cleaved caspase-3 was evident in mainly GCL (*arrows*) and INL (*star*) at 24 h after I/R in the NS I/R retina. WD-Hpt prevented this reaction. *GCL* ganglion cell layer, *IPL* inner plexiform layer, *INL* inner nuclear layer, *OPL* outer plexiform layer, *ONL* outer nuclear layer. *Scale bar* 200 μm (*left line*) and 100 μm (*middle line*).

Fig. 6

TUNEL labeling of retinal sections at 3 days after I/R. **a** Representative cropped images of the retina in four groups. TUNEL-positive cells were increased in the GCL and INL of the NS I/R retina ($^{**}P < 0.01$ vs NS con). WD-Hpt treatment decreased the number of TUNEL-positive cells (††$P < 0.01$ vs NS I/R). TUNEL-positive cells were hardly confirmed in both the NS con and WD-Hpt con retina. *Scale bar* 100 μm. **b** A graph shows the average number of TUNEL-positive cells in the whole retinal sections.

Fig. 7

Western blot for ERK involved in the neuronal cell death during I/R. Phosphorylation of ERK was increased in the NS I/R retina compared to control retina. In contrast, the phosphorylation was reduced by WD-Hpt treatment ($n = 3$; $^{**}P < 0.01$ vs NS con; ††$P < 0.01$ vs NS I/R).

Figure1

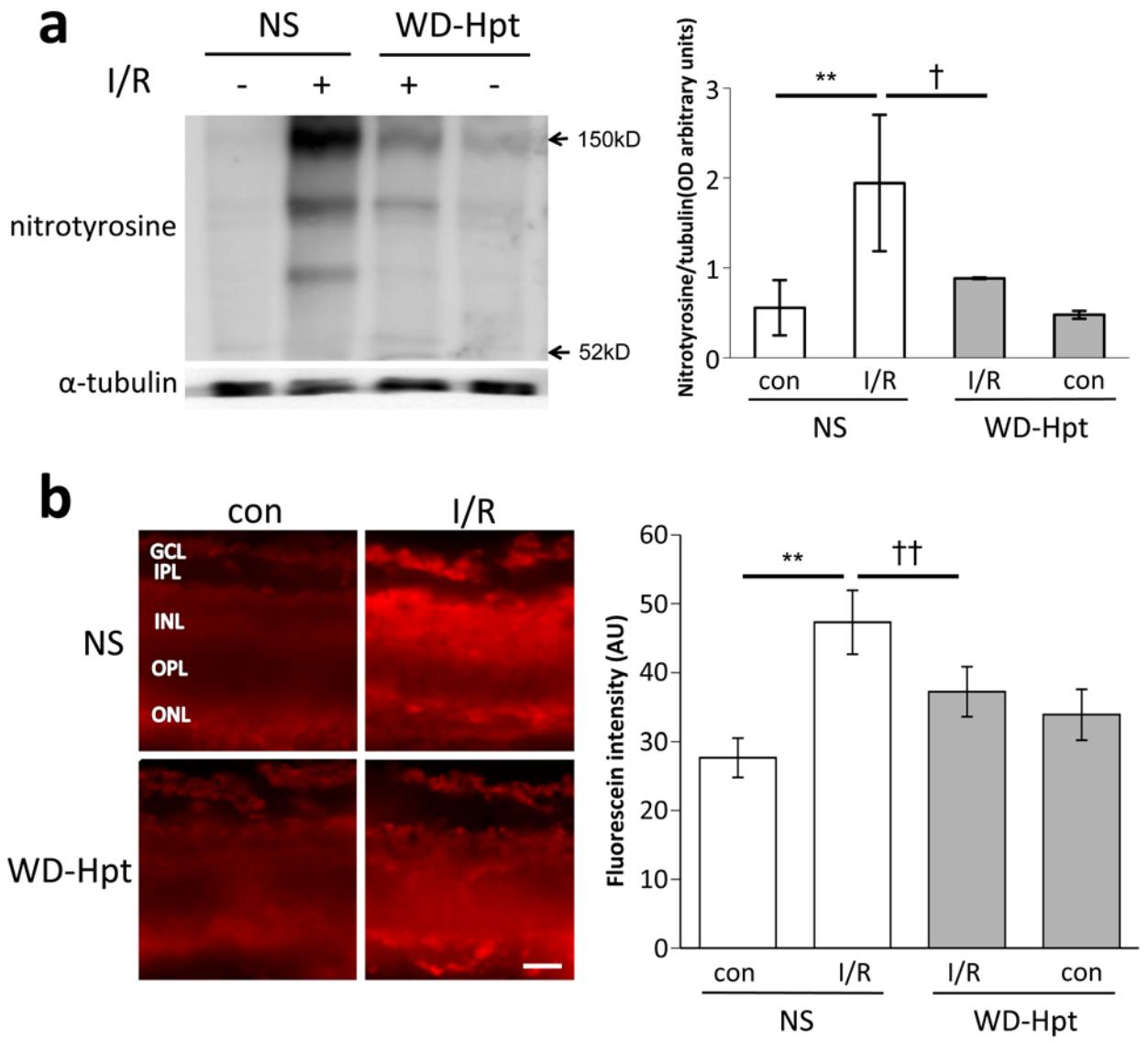
a
NS
WD-Hpt
I/R
- + + -
150kD
52kD
nitrotyrosine
α-tubulin
Nitrotyrosine/tubulin(OD arbitrary units)
**
†
con
I/R
I/R
con
NS
WD-Hpt
b
con
I/R
GCL
IPL
INL
OPL
ONL
NS
WD-Hpt
Fluorescein intensity (AU)
**
††
con
I/R
I/R
con
NS
WD-Hpt

Figure2

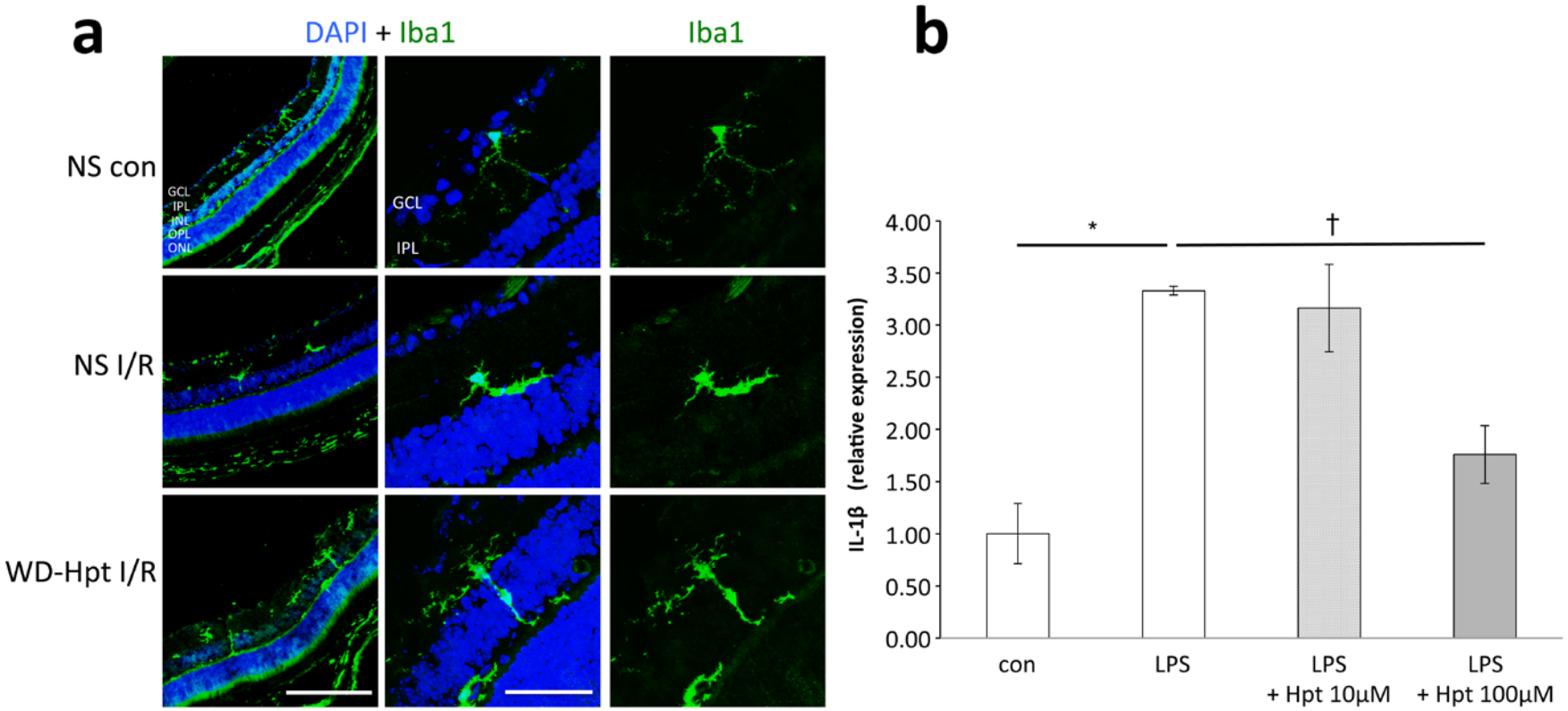
a
DAPI + Iba1
Iba1
NS con
NS I/R
WD-Hpt I/R
GCL
IPL
INL
OPL
ONL
GCL
IPL
b
IL-1β (relative expression)
4.00
3.50
3.00
2.50
2.00
1.50
1.00
0.50
0.00
*
†
con
LPS
LPS
+ Hpt 10μM
LPS
+ Hpt 100μM

Figure3

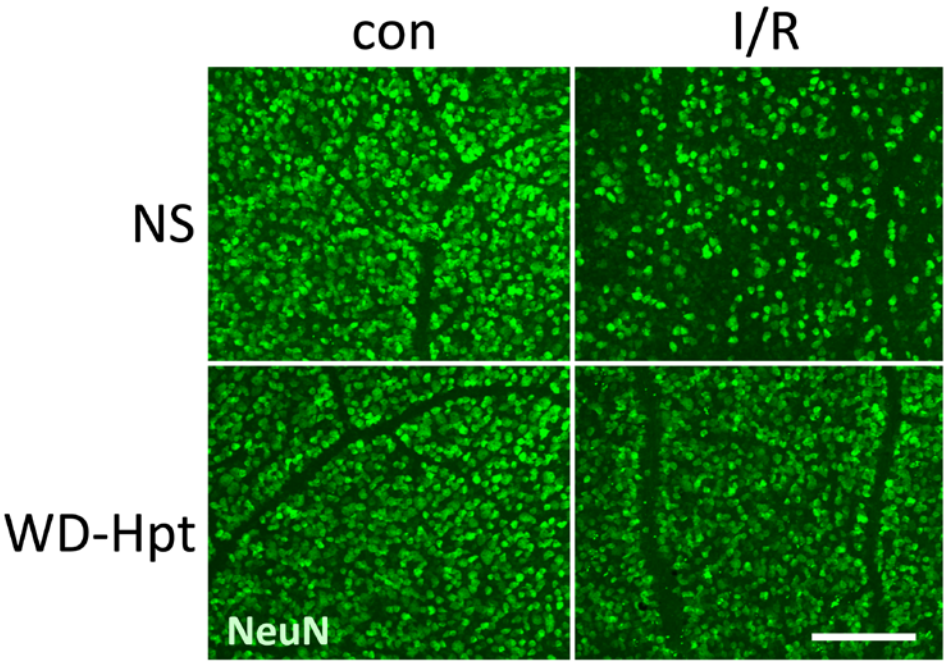
con
I/R
NS
WD-Hpt
NeuN

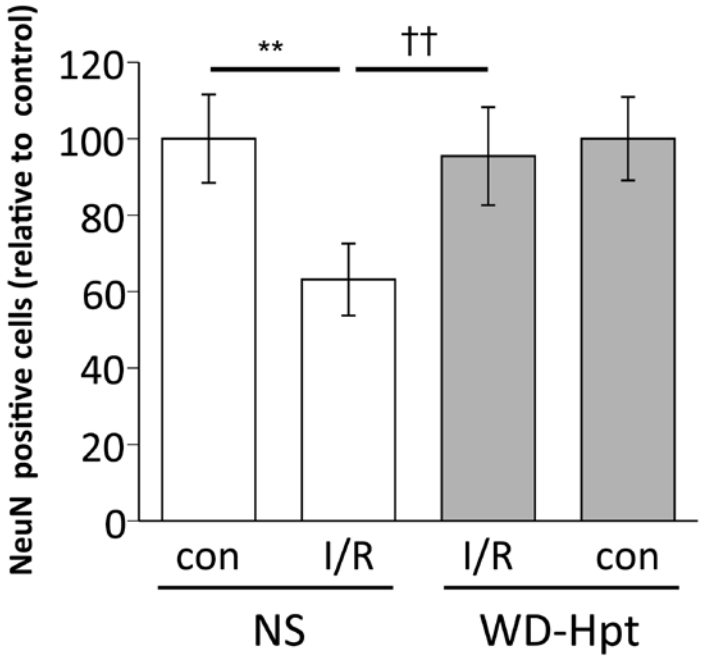
NeuN positive cells (relative to control)
120
100
80
60
40
20
0
**
††
con
I/R
I/R
con
NS
WD-Hpt

Figure4

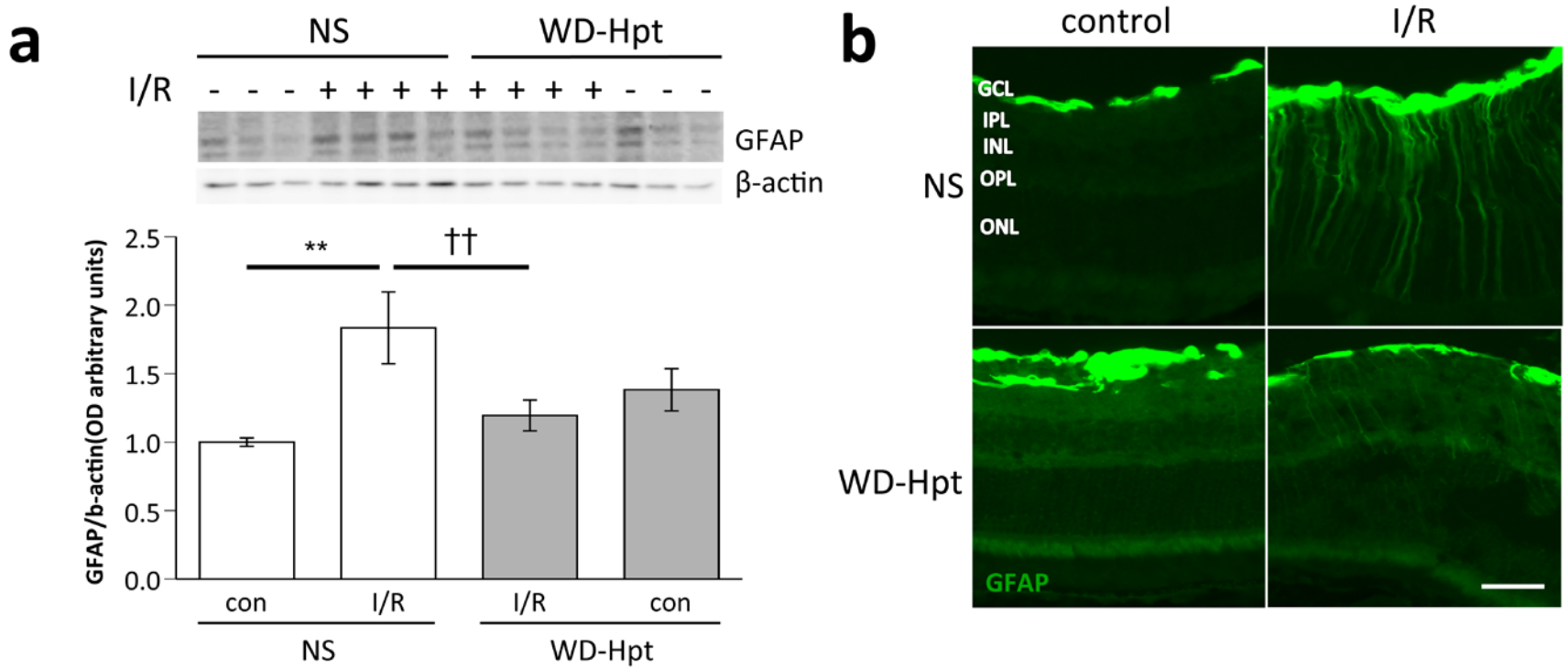
a
NS
WD-Hpt
I/R
- - - + + + + + + + + - - -
GFAP
β-actin
GFAP/b-actin(OD arbitrary units)
2.5
2.0
1.5
1.0
0.5
0.0
**
††
con
I/R
I/R
con
NS
WD-Hpt
b
control
I/R
GCL
IPL
INL
OPL
ONL
NS
WD-Hpt
GFAP

Figure5

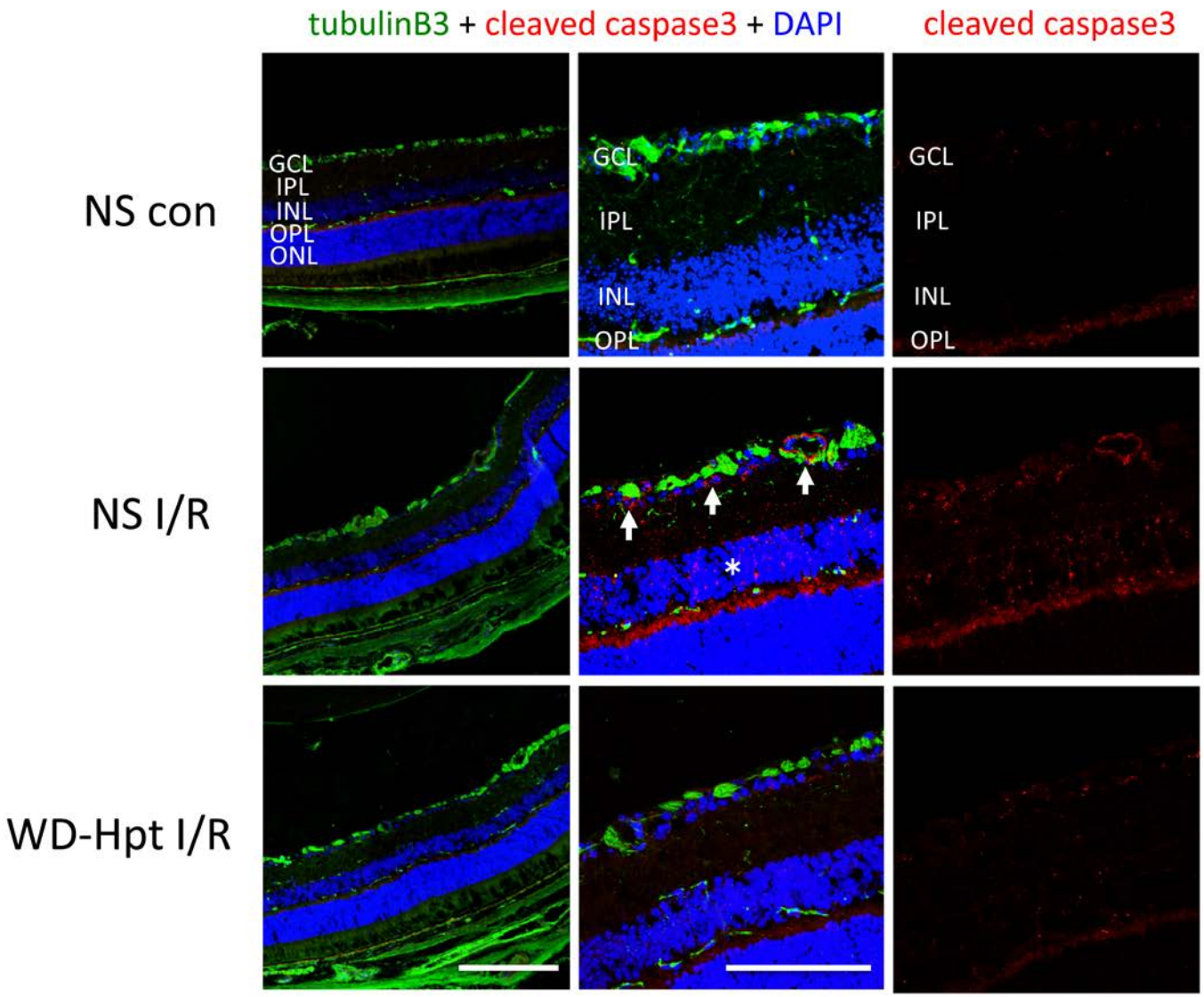
tubulinB3 + cleaved caspase3 + DAPI
cleaved caspase3
NS con
NS I/R
WD-Hpt I/R
GCL
IPL
INL
OPL
ONL

Figure6

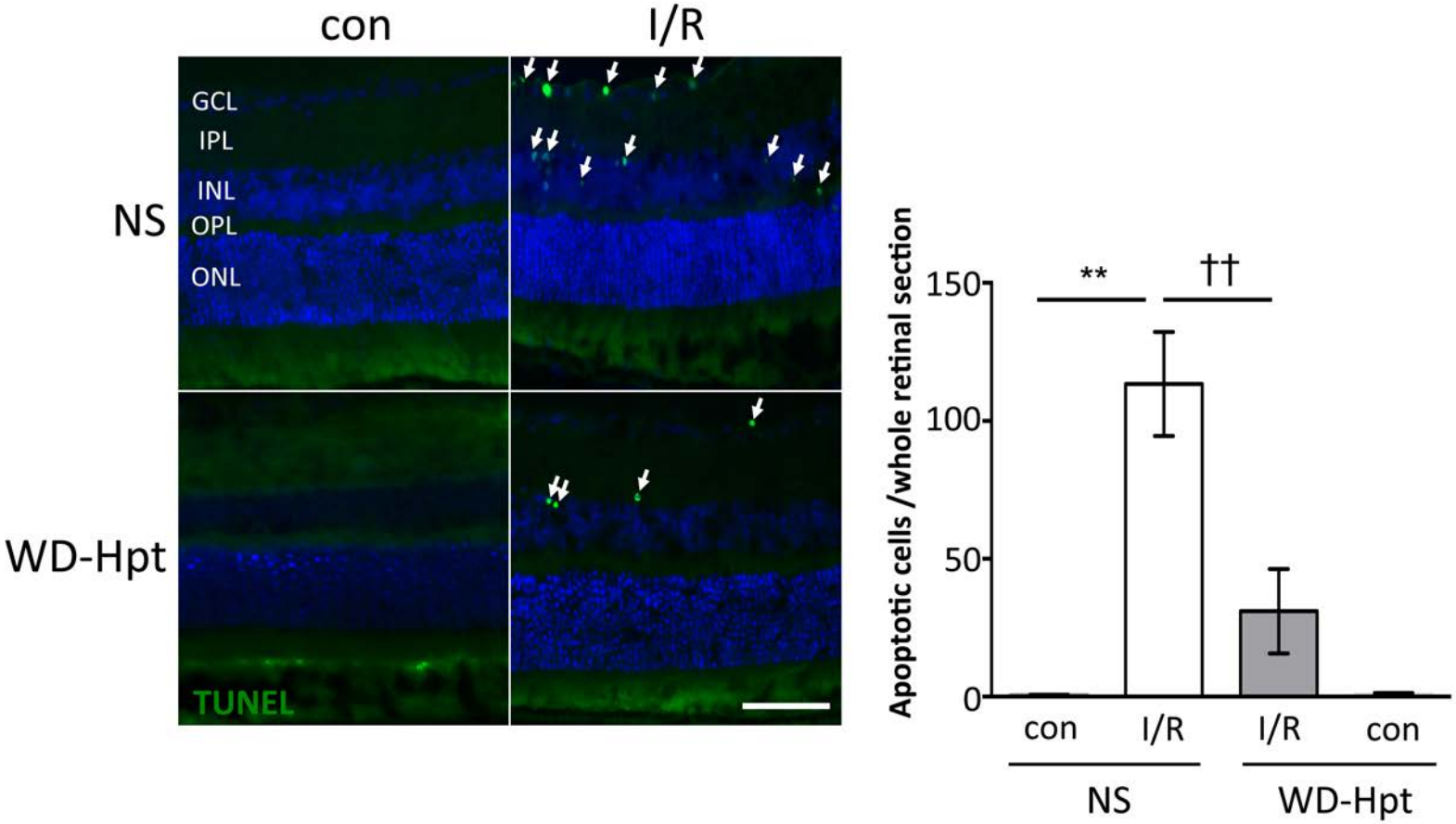
con
I/R
NS
WD-Hpt
GCL
IPL
INL
OPL
ONL
TUNEL
Apoptotic cells /whole retinal section
150
100
50
0
**
††
con
I/R
I/R
con
NS
WD-Hpt

Figure7

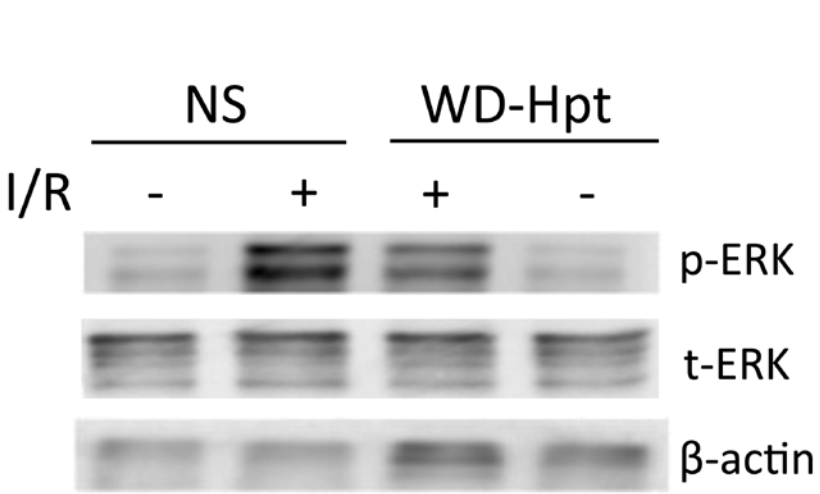
NS
WD-Hpt
I/R
-
+
+
-
p-ERK
t-ERK
β-actin

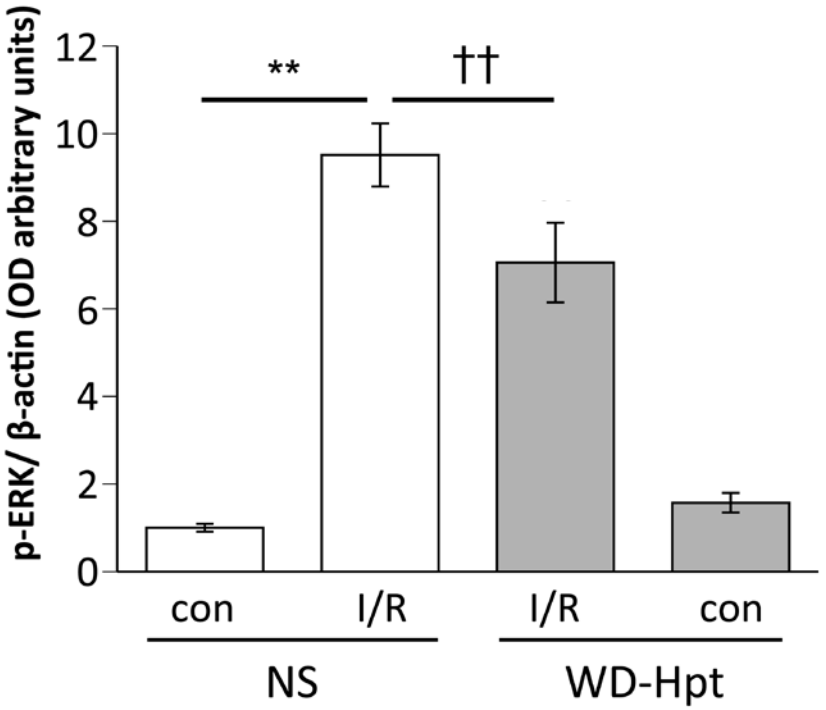
p-ERK/ β-actin (OD arbitrary units)
12
10
8
6
4
2
0
**
††
con
I/R
I/R
con
NS
WD-Hpt